

# OCEAN EVAPORATION AND PRECIPITATION AT REGIONAL AND GLOBAL SCALE IN THE HOAPS SATELLITE CLIMATOLOGY AND OTHER DATA SETS

Stephan Bakan<sup>(1)</sup>, Axel Andersson<sup>(2)</sup>, Christian Klepp<sup>(2)</sup>, Daniel Klocke<sup>(1)</sup>, Jörg Schulz<sup>(3)</sup>

<sup>(1)</sup> Max Planck Institute for Meteorology, Bundesstr. 53, D-20146 Hamburg (Germany),  
Email: [stephan.bakan@zmaw.de](mailto:stephan.bakan@zmaw.de); [daniel.klocke@zmaw.de](mailto:daniel.klocke@zmaw.de)

<sup>(2)</sup> Meteorological Institute, University of Hamburg, Bundesstr. 55, D-20146 Hamburg (Germany), Email:  
[axel.andersson@zmaw.de](mailto:axel.andersson@zmaw.de); [christian.klepp@zmaw.de](mailto:christian.klepp@zmaw.de)

<sup>(3)</sup> German Weather Service (DWD), CM-SAF, Frankfurter Straße 135, 63067 Offenbach (Germany), Email:  
[joerg.schulz@dwd.de](mailto:joerg.schulz@dwd.de)

## ABSTRACT

The HOAPS satellite data set contains, besides several other water cycle variables, global fields of evaporation, precipitation and the net freshwater flux over the ice-free ocean for the interval 1988-2005. The data fields show all the known global climatological features and regional details. Average values and temporal development of precipitation and evaporation compare well with other established satellite data sets. Due to essentially trend-free global average precipitation and increasing evaporation, E-P increases with time, being about twice as large as the documented global continental runoff. The spatial trend distribution hints at an intensification of the Hadley circulation and of the general water cycle with time.

Comparison with widely used reanalysis fields exhibit remarkable similarities and differences in the temporal development of evaporation and precipitation and the resulting E-P balance over global oceans. The ERA globally averaged E-P products are not in balance with continental runoff and change systematically with time. On the other hand, as the globally averaged NCEP evaporation and precipitation both increase with time very similarly, this results in a nearly constant E-P in near balance with the global run-off. More detailed analysis will be necessary to understand the different results and issues involved.

As an application example, a combined HOAPS and GPCC data product is used to document the response of regional and global precipitation and other water cycle components to the North Atlantic Oscillation in rather high spatial resolution.

## 1. INTRODUCTION

Proper knowledge of the global water cycle is crucial for the understanding and successful modelling of the global climate system. However, a reliable measurement of essential water cycle components with sufficient spatial and temporal coverage, especially over the global oceans, became only possible since the advent of satellite platforms with microwave detectors in space. This spectral range is well suited for the derivation of atmospheric parameters such as water vapor or liquid water as well as for the retrieval of relevant freshwater flux components at the ocean surface.

Especially since the availability of the Special Sensor Microwave Imager (SSM/I) on the satellites of the Defense Meteorological Satellites Program (DMSP) in the late 1980s, long-term global fields of water cycle related quantities have been derived and augmented by various additional data sources for special application purposes. Generally, these data sets provide either surface fluxes or precipitation estimates. An extensive overview of satellite derived air-sea flux data sets including detailed intercomparisons will be given in [1]. In addition, reference [2] provides a comprehensive introduction to the current state of the art precipitation algorithms and products and related validation and modelling aspects. In principle, the satellite retrieved data sets could be combined to estimate the global ocean freshwater flux. This would be highly required but is also a difficult task, as different data sources have to be combined while there is no comprehensive in-situ validation data available [3].

The Hamburg Ocean Atmosphere Parameters and Fluxes from Satellite Data (HOAPS) is the first generally available compilation of both precipitation and evaporation from one consistently derived global satellite product [4]. Based on multi-satellite averages, inter-sensor calibration, and an efficient

sea ice detection procedure, HOAPS provides a climatological data set of ocean latent heat flux and precipitation from satellite data for a climatological assessment of crucial water cycle processes over the global oceans.

The present paper contains a short overview of HOAPS features, some intercomparisons and first results with an application example.

## **2. HOAPS**

The HOAPS-3 climatology contains fields of precipitation, surface fluxes and related atmospheric parameters over the global ice-free ocean between 1987 and 2005. The climatology and the methodology to derive it from satellite data is described in detail in [4].

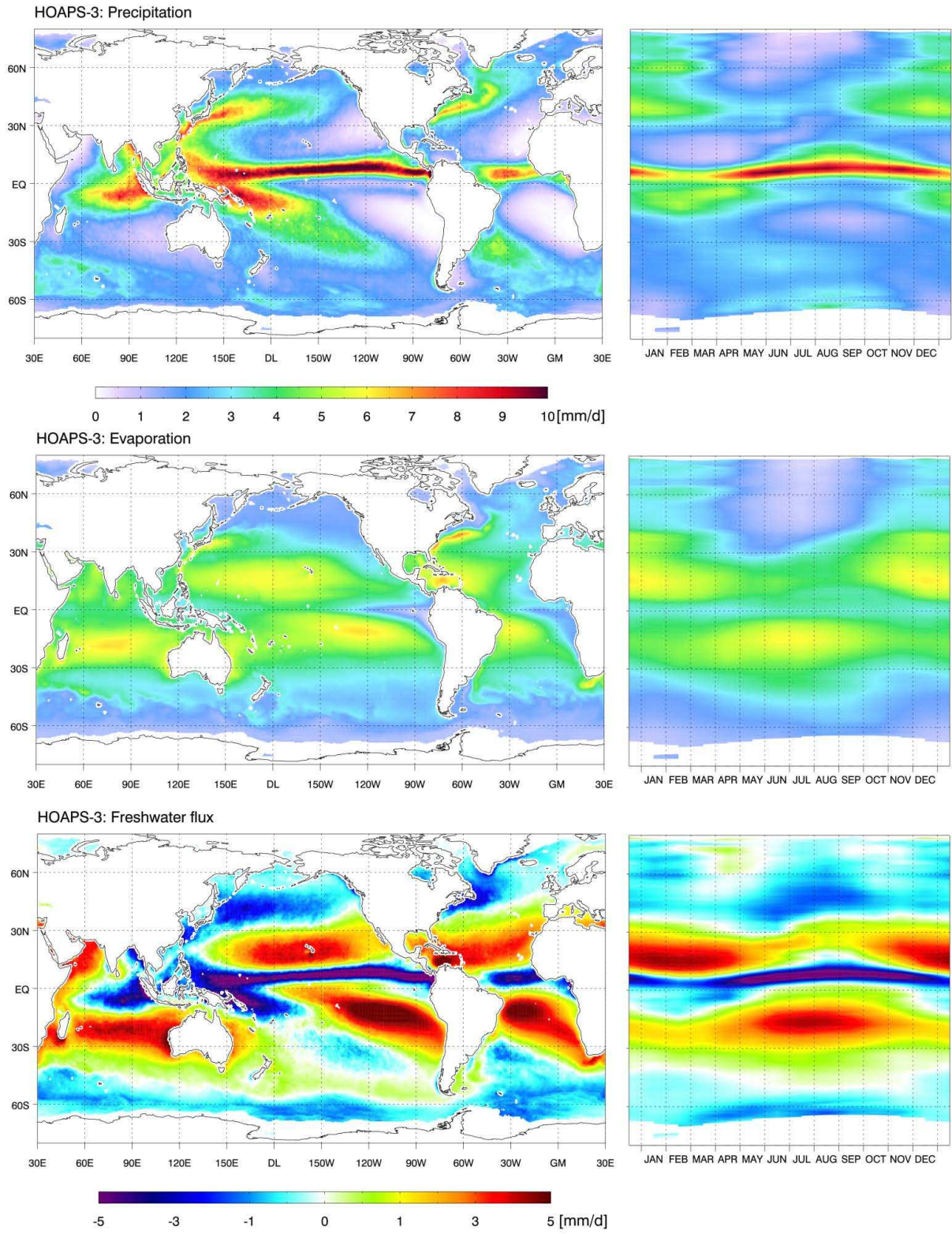


Figure 1. Climatological mean fields (left column) and yearly cycle (right column) of HOAPS-3 precipitation (top), evaporation (mid) and freshwater flux (bottom) for the years 1988 to 2005.

Passive microwave data from the SSM/I instrument, operating on the polar orbiting DMSP satellites, are used to retrieve basic variables. From these individual components of surface fluxes of heat, evaporation, and precipitation are derived. These data as well as the resulting net freshwater flux (E-P) fields are provided on a half degree grid through [www.hoaps.org](http://www.hoaps.org).

A specific goal of the HOAPS effort was to generate a global ocean product for climatological studies from satellite based data. Therefore, great care was put into inter-sensor-calibration between the different DMSP satellites. All HOAPS variables are derived from brightness temperature of the SSM/I radiometers. Only the additionally needed SST information is taken from the NODC/RSMAS Pathfinder SST data set which uses AVHRR data [5]. To avoid data contamination through sea ice in the individual pixels, a sea ice detection procedure based on the NASA Team algorithm has been applied [6].

HOAPS latent heat flux retrieval is based on the bulk aerodynamics COARE 2.6a algorithm described in [7] and [8]. This requires atmospheric specific humidity (implemented after [9]) and sea surface saturation specific humidity as well as near surface wind speed. The latter as well as the precipitation in HOAPS are directly retrieved from the SSM/I measurements by a neural network approach.

As Fig. 1 shows, the mean fields and yearly cycles of HOAPS-3 (1988-2005) for precipitation, evaporation and freshwater flux reproduce the known climatological features. In particular, the well expressed ITCZ and the warm pool precipitation, the subtropical evaporation maxima, and the hydrological maxima over the warm Gulfstream and Kuroshio ocean currents catch the observer's attention.

On a global scale, the average evaporation in HOAPS-3 exceeds rain rate over the ocean systematically with almost negligible yearly cycle and small monthly variations. Globally averaged precipitation over the ice free ocean is slightly increasing during the available 18 years of HOAPS, although this trend is not highly significant.

Regionally, a substantial increase in the ITCZ and over the southern mid latitude oceans is somewhat compensated by reductions in the subtropics and no significant change over the northern oceans.

A detailed uncertainty description for the satellite based HOAPS fluxes is difficult due to the lack of reliable and comprehensive in situ data. However, studies demonstrated the quality of some aspects of

the HOAPS evaporation and precipitation products (e.g. [10] and [11]).

### 3. INTERCOMPARISONS

#### 3.1. Precipitation

Fig. 2 shows the comparison of zonal means (top panel) and monthly global means (bottom panel) of HOAPS precipitation with several other satellite and reanalysis products. For zonal means, satellite products exhibit generally a similar behaviour with some exceptions in mid to high latitudes. Reanalysis products tend to provide comparatively high tropical precipitation and an intense southern ITCZ.

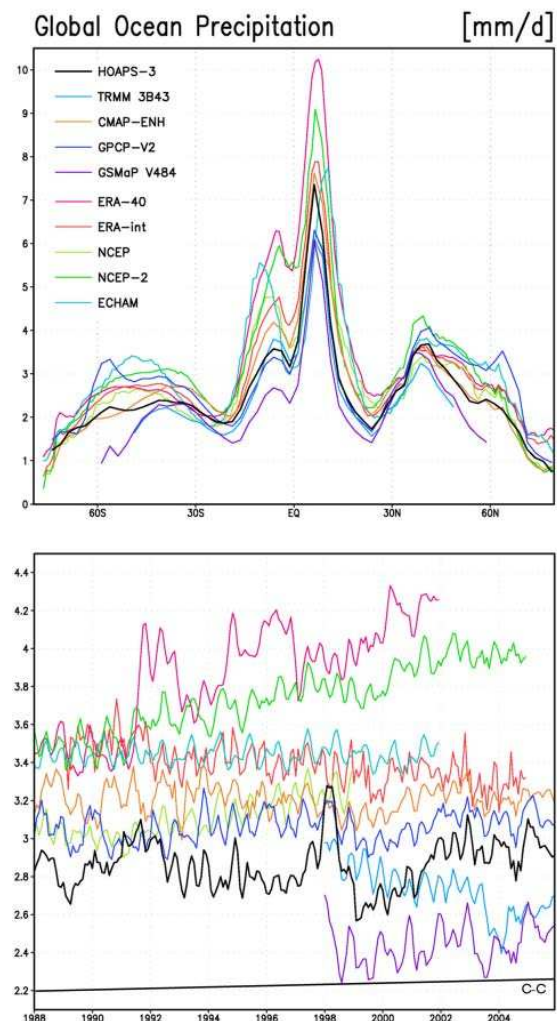


Figure 2. Comparison of zonal means (top panel) and monthly global means (bottom panel) of HOAPS precipitation with several other satellite and reanalysis

products. The line labelled C-C roughly indicates the hypothesized trend of water cycle intensity of 7% per degree SST.

The temporal development of HOAPS precipitation (Fig. 2, bottom panel) compares well with other satellite climatologies as e.g. GPCP-V2 or CMAP, both of which have insignificant temporal trends at somewhat higher but less variable values. A conspicuous minimum in the HOAPS evaporation time series in 1991 is related to impaired accuracy of the SST data for several months after the eruption of Mt. Pinatubo.

In comparison with reanalysis data we find, that both available NCEP reanalyses exhibit a substantial increase of precipitation over the global ocean after 1987. ERA40 data show an even stronger increase, which has been known for some time to be erroneous [12]. The recalculation in the ERA-interim project results now in similar but with time slightly decreasing average precipitation rates over the global ocean.

In reference [13] the idea has been put forward, that due to the increase of the atmospheric water vapour saturation mixing ratio by about 7% per degree increase of temperature (according to the Clausius-Clapeyron equation), various atmospheric water cycle components could be expected to increase by about 7% per degree increase of global average SST (according to the Clausius-Clapeyron equation). Although statistically not highly significant, this is almost exactly the value of the nominally calculated linear trend for the globally averaged HOAPS precipitation (see the black lines labelled HOAPS and C-C in Fig. 2).

### 3.2. Evaporation

The intercomparison for the zonally and globally averaged evaporation over ocean is displayed in Fig. 3. All data sets show fairly similar zonal mean evaporation. HOAPS exhibits a substantial increase during the study period, which results mainly from the increase in wind speed and in sea-air difference of specific humidity in the subtropics. The related linear trend is substantially higher than would have been expected from the above mentioned Clausius-Clapeyron-criterion (cf. line labelled C-C in Fig. 3) for yet unexplained reasons. Comparison with other satellite-derived evaporation products, among them e.g. the J-Ofuro V2 and the IFREMER V3 data sets, results in fairly similar values, variability and trend behavior. Especially noticeable is the very similar

time behavior of the NOCS V2 data set, which is estimated from a completely different data set, namely the ICOADS ship measurements. Only the recently published OAFlux V3, which is a blending of satellite and reanalysis data, exhibits a substantially smaller increase with time.

Global evaporation in various reanalysis data sets show strongly different temporal behavior. While globally averaged ocean evaporation from both NCEP reanalyses increases with time at approximately the same rate as in HOAPS, both ERA reanalyses exhibit insignificant long-term trends.

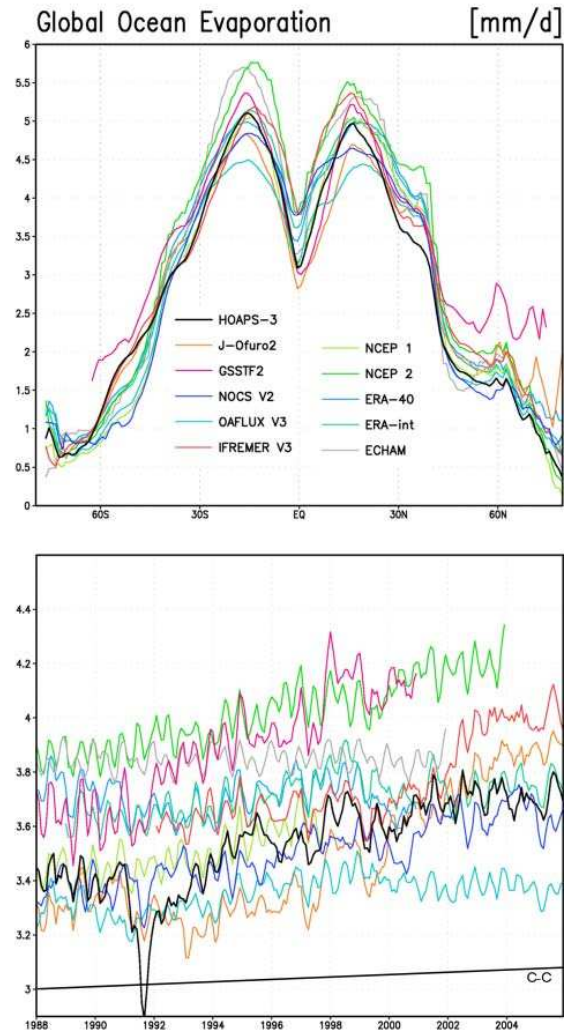


Figure 3. Comparison of zonal means (top panel) and monthly global means (bottom panel) of HOAPS evaporation with several other satellite and reanalysis products

### 3.3. Freshwater flux

Only a very few of the considered data sets provide also fields of the ocean freshwater flux and its time development. While this is readily available from reanalyses and model data, among the satellite based data sets to day only HOAPS provides this ocean surface water balance quantity. Fig. 4 shows the globally averaged monthly mean values of freshwater flux (evaporation – precipitation) between 1988 and 2005 together with the seasonal range of continental runoff from NCEP. The data reflect generally the expected average preponderance of evaporation over precipitation over the global oceans. Only the ERA40 data exhibit substantially negative freshwater fluxes due to the mentioned problems with the precipitation component. For a few months after the Pinatubo eruption in late 1991 also the HOAPS freshwater flux turns negative, which is mostly due to insufficiently corrected Pathfinder SST data during that time. Otherwise, all reanalysis products exhibit freshwater values in the early part of the comparison period that fit reasonably to the continental runoff distributed with the NCEP reanalysis data, but differ with time more and more. While the freshwater flux from both NCEP data sets remain fairly constant with time, ERA-interim increases at the same rate as HOAPS does. Both products seem to be substantially off the nominal continental runoff towards the end of the intercomparison period.

For completeness, Fig. 4 contains also the time development of the freshwater flux in the ECHAM IPCC climate model run (mean of 3 ensemble members) for the 20th century (1988-2001). In this case non of the three quantities, average precipitation, evaporation and resulting freshwater flux over the global ocean, exhibits any obvious and significant trend during the 13 available model years.

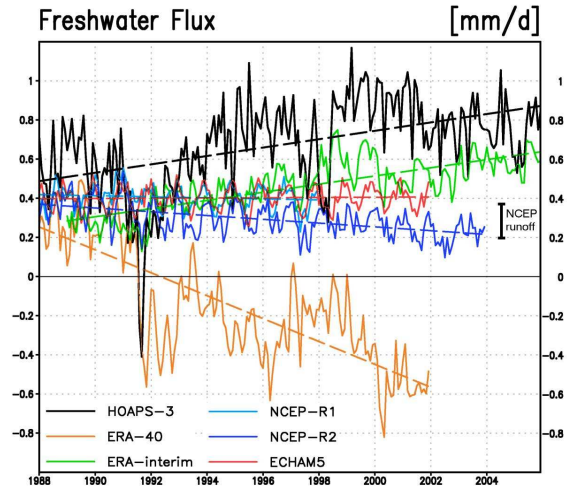


Figure 4. Monthly mean global average freshwater flux between 1988 and 2005 for several data products together with the seasonal range of NCEP continental runoff

Although not fully closed with respect to the global river runoff, the HOAPS-3 global net freshwater flux estimate over the ocean lies within 10% of the individual E and P estimates. However, locally larger uncertainties remain mostly in regions with high variability or particular atmospheric conditions.

### 4. NORTH ATLANTIC OSCILLATION

The HOAPS climatology has been applied to study the influence of the North Atlantic Oscillation (NAO) on regional and global water cycle components. It is well known, that one of the most important influences on the decadal variability of the European climate comes from the NAO, which is the dominating pattern of atmospheric variability in the northern hemisphere. It is characterized by the sea-level pressure difference between the Icelandic Low and the Azores High. In consequence, fields of wind speed, precipitation and various other atmospheric quantities exhibit significant related variability pattern. The strength and phase of the NAO has been described with different indices. In the following, a station based index is used, that represents essentially the normalized pressure difference between Iceland and Lisbon.

During the 18 years of the HOAPS time the series, the NAO index has gone through almost it's whole span of positive as well as negative monthly average values. Therefore, we analyzed the HOAPS fields with respect to this NAO index variability during

winter months, in which the NAO signal is strongest. The analysis is based on 72 winter months (Dec-Mar) between 1988 and 2005.

To show more clearly the extension of variations over land, a quasi-global precipitation field coverage has been constructed by combining HOAPS-3 with an available land precipitation data set. It is the „Full Reanalysis Version 4“ data set from the GPCP (Global Precipitation Climatology Center) at DWD (the German Weather Service), which is compiled from rain gauge data. This combined data set covers most of the global land and sea areas with the exception of sea ice covered regions (e.g. Arctic and Labrador Sea area). It turned out, that the two precipitation fields from two completely independent data sources fit surprisingly well together without exhibiting obvious jumps and inhomogeneities across coastlines. Details of this procedure and the related analysis will be published in [14]. The following discussion will concentrate on precipitation.

Fig. 5 shows as an example the composite field of precipitation difference between the upper and lower quartile of NAO index values during the winter months between 1988 and 2005. The difference field exhibits the enhanced precipitation especially in the eastern part of the North Atlantic storm track, extending far into northern and northeastern Europe during phases of high NAO index. The strong increase of precipitation along the western coasts of the British Isles and of Norway is contrasted by a rather decrease of precipitation over the North Sea and even the Baltic Sea. At the same time, precipitation decreases significantly over the whole of Southern Europe between far out over the Atlantic Ocean and the eastern territories of Turkey. Another significant decrease is documented around the Labrador Sea area.

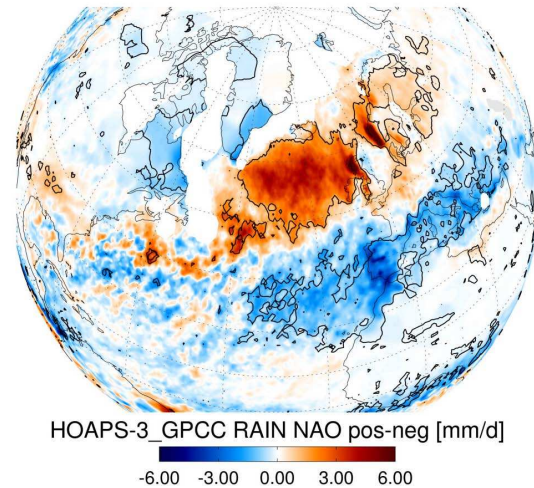


Figure 5. Composite field of precipitation difference between cases in the upper and lower quartile of the NAO index values with an indication of areas of significant changes

In Fig. 6 the correlation of the global precipitation field with the NAO index is displayed. Besides the high correlation, over Europe and the North Atlantic, a considerable distance of influence is displayed in consistence with results from the ERAinterim reanalysis (not shown). The area of strongly positive correlation extends from the North-Atlantic and Europe far into Eastern Siberia and on the other side across the southern US area deep into the subtropical Pacific. The patches of significantly negative correlations over the tropical Africa and of positive correlations over the tropical Indian Ocean appear also in the parallel analysis of ERA-interim data. To which extent even the patches of correlation over the southern ocean are really considerable remains open at the moment, although some of these patches are also found in the ERA-interim reanalysis.

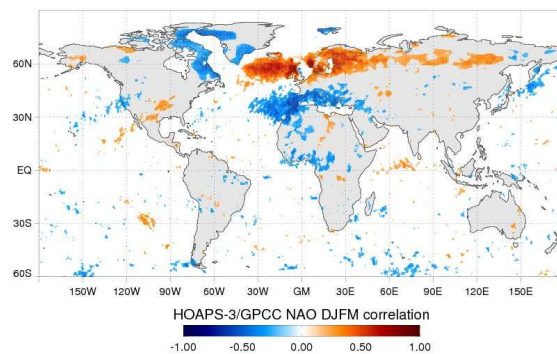


Figure 6. Global distribution of the significant parts of the correlation between HOAPS/GPCC precipitation and the NAO index

## 5. CONCLUSIONS

The HOAPS satellite climatology of several essential water cycle components over the ice free global ocean, exhibits the known global climatological features and regional details. Values and trends for precipitation and evaporation compare well with other established satellite data sets.

Precipitation remained essentially constant between 1988 and 2005, while evaporation increased by about 7% per decade, mostly due to wind and SST increase in the subtropical regions. E-P increases accordingly and is about two times larger than the documented global continental runoff. The spatial trend distribution hints at an intensification of the Hadley circulation and of the general water cycle with time.

Comparison with other widely used satellite and reanalysis fields exhibit remarkable similarities and differences in the temporal development of evaporation and precipitation and the resulting E-P balance over global oceans. ERA40 shows an implausible decrease of E-P, while it increases in ERAinterim similar to HOAPS. NCEP evaporation increases with time very similar to HOAPS, but as precipitation increases also considerably, E-P is nearly constant with time in near balance with the global run-off. Spatial pattern also turn out to be in parts substantially different among the various data sets. More detailed analysis will be necessary to understand the different results and issues involved.

As an application example, the combined HOAPS/GPCC data document the response of regional and global precipitation and other water cycle components to the North Atlantic Oscillation in higher detail than was usual hitherto.

HOAPS 3 is publicly available from [www.hoaps.org](http://www.hoaps.org). In near future, some of the core HOAPS products will be routinely derived and provided by the EUMETSAT Satellite Application Facility on Climate Monitoring (CM-SAF, [www.cmsaf.eu](http://www.cmsaf.eu)) at the German Weather Service DWD.

## ACKNOWLEDGEMENTS

This research was funded by the German Science Foundation (DFG) under grant SFB 512 "Cyclones and the North Atlantic climate system" and by the Helmholtz Foundation through the Virtual Institute

project "Investigation of extratropical cyclones using passive and active microwave radars". Several of the comparison data sets were gratefully obtained from the project websites.

## REFERENCES

1. Clayson, C. A., et al. (2010): Results of the seaflux intercomparison project. In prep.
2. Levizzani, V., P. Bauer & F. Turk (2007). Measuring Precipitation from Space: EURAIN-SAT and the Future. *Advances in Global Change Research*, Vol. 28. Springer Verlag, 722 pp.
3. Schlosser, C. A. & P. R. Houser (2007). Assessing a satellite-era perspective of the global water cycle. *J. Climate*, 20 (7), 1316–1338.
4. Andersson, A., Klepp, C., Fennig, K., Bakan, S., Graßl, H. & Schulz, J. (2010). The HOAPS climatology: Essential water cycle components over the global ice-free ocean from satellite data. submitted to *J. Appl. Meteor. Climatol.*, in review.
2. Berry, D. I. & E. C. Kent (2009). A new air–sea interaction gridded dataset from ICOADS with uncertainty estimates. *Bull. Amer. Meteor. Soc.*, 90, 645–656.
5. Kenneth, S. C. (2004). Global AVHRR 4 km SST for 1985–2001, Pathfinder V5.0, NODC/RSMAS. *Tech. rep.*, NOAA National Oceanographic Data Center, Silver Spring, Maryland. NODC Accession Numbers 0001763-0001864: Pathfinder AVHRR Version 5.0.
6. Swift, C. T., Fedor, L. S. & Ramseier, R. O. (1985). An algorithm to measure sea ice concentration with microwave radiometers. *J. Geophys. Res.-Oceans* 90, 1087–1099.
7. Fairall, C. W., Bradley, E. F., Rogers, D. P., Edson, J. B. & Young, G. S. (1996). Bulk parameterization of air-sea fluxes for Tropical Ocean-Global Atmosphere Coupled-Ocean Atmosphere Response Experiment. *J. Geophys. Res.-Oceans* 101, 3747–3764.
8. Fairall, C. W., Bradley, E. F., Hare, J. E., Grachev, A. A. & Edson, J. B. (2003). Bulk parameterization of air-sea fluxes: Updates and verification for the COARE algorithm. *J. Climate* 16(4), 571–591.
9. Bentamy, A., K. B. Katsaros, A. M. Mestas-Nunez, W. M. Drennan, E. B. Forde & H. Roquet (2003). Satellite estimates of wind speed and latent heat flux over the global oceans. *J. Climate* 16(4), 637–656.
10. Bourras, D. (2006). Comparison of five satellite-derived latent heat flux products to moored buoy data. *J. Climate*, 19 (24), 6291–6313.
11. Klepp, C., Bumke, K., Bakan, S. & Bauer, P. (2009). Ground validation of oceanic snowfall in satellite climatologies during LOFZY. submitted to *Tellus A*, in review.

12. Simmons, A., S. Uppala, D. Dee & S. Kobayashi (2007). ERA–Interim: New ECMWF reanalysis products from 1989 onwards. *ECMWF Newsletter*, **110**, 25–35.
13. Wentz, F. J., L. Ricciardulli, K. Hilburn & C. Mears (2007). How much more rain will global warming bring? *Science*, **317** (5835), 233–235.
14. Andersson, A., S. Bakan, H. Graßl (2009). Satellite derived North Atlantic precipitation and freshwater flux variability with special emphasis on the North Atlantic Oscillation. Submitted to *Tellus A*.